Polyhedron 117 (2016) 703–709

Contents lists available at ScienceDirect

Polyhedron

journal homepage: www.elsevier.com/locate/poly

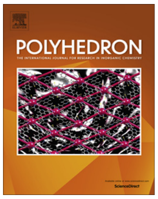

Lanthanide(III) based metal organic frameworks constructed from 5-nitroisophthalate ligand with 2,4,5-tri(4-pyridyl)-imidazole templates: Syntheses, structures, and luminescent properties

Dao-Jun Zhang [a], You-Zhu Yu [b], Jun-Jie Wang [a,*], Er-Ni Wang [a], Feng Jin [a], Meng-Yao Zhang [a], Hui-Na Huang [a], Qing-Qing Zhao [a], Yun-Feng Shi [a,*]

[a] College of Chemistry and Chemical Engineering, and Henan Key Laboratory of New Optoelectric Functional Materials, Anyang Normol University, Anyang, Henan 455000, China
[b] College of Chemistry and Environmental Engineering, Anyang Institute of Technology, Anyang, Henan 455000, China

ARTICLE INFO

Article history:
Received 26 May 2016
Accepted 2 July 2016
Available online 13 July 2016

Keywords:
5-Nitroisophthalic acid
2,4,5-Tri(4-pyridyl)-imidazole
La(III) and Nd(III) metal–organic frameworks
Template effect
Luminescent properties

ABSTRACT

Two unprecedented Ln-based metal–organic frameworks (MOFs) based on 5-nitroisophthalic acid ($H_2\mathbf{L}$) and 2,4,5-tri(4-pyridyl)-imidazole (Htpim), namely $\{[H_3tpim][Ln_2(\mathbf{L})_4(H_2O)]\}_n$ [Ln = La (**I**), Nd (**II**)], were prepared by solvothermal reactions and characterized by IR, elemental analysis and X-ray diffraction analysis. X-ray single crystal diffraction indicates that complexes **I** and **II** display similar 2D 4^4 frameworks with similar tetranuclear $[Ln_4(COO)_{16}(H_2O)_2]$ secondary building units due to the effect of Ln contraction and the same coordination modes of **L** ligands as well as the template effect of Htpim. Moreover, thermal stabilities and luminescent properties of **I** and **II** were also investigated.

1. Introduction

In the past decades, the rational design and synthesis of metal–organic frameworks (MOFs) based upon assembly of organic ligands and metal ions have attracted considerable attention for their interesting architectures and tailor-made applications in optics, magnetism, gas storage, ion exchange, and catalysis, etc. [1–6]. Now, the utilization of pillars as secondary building units has proven to be a versatile strategy in the construction of MOFs, especially highly porous structures [7–10]. As typical pillars, aromatic carboxylate ligands, such as phthalic, isophthalic, terephthalic, and trimesic acid, have been extensively investigated in past decades due to their strong coordination capability, their large conjugated systems, and the possibility of offering new functional materials [11–15]. Moreover, in view of the previous reports, we found that different substituted groups on the multicarboxylate ligands may have an influence on the assembling processes, the structures and even the properties of MOFs due to their geometric and electronic effects [16,17]. On the other hand, besides the pillar ligands, many other components such as coligands or templates also play a crucial role in the formation of MOFs. In general, on the basis of previous reports, the coligands coordinate to metal centers as ancillary ligands while the templates (being neutral or charged) do not coordinate to metal centers but occupy specific space and interact with other components via weak interactions in the final structures. Especially for some coligands, for instance, multidentate N-donor ligands are facile to protonate or deprotonate and can act as templates to guide the formation of anionic or cationic MOFs with special structures [18–20].

Moreover, differing from transition-metal ions, the lanthanide (Ln) analogues are highly sought after because Ln ions possess high coordination numbers, flexible coordination geometries, and the effect of Ln contraction that can afford structural diversity [21,22]. Meanwhile, Ln-based MOFs can show distinct characteristic luminescent emissions and large anisotropic magnetic moments arising from a large number of spins and strong spin–orbit coupling, which are much different from those of transition-metal-based MOFs [23].

However, to the best of our knowledge, Ln-based MOFs of a multicarboxylate containing 2,4,5-tri(4-pyridyl)-imidazole (Htpim) have not yet been reported. We decided to construct Ln-based MOFs with mixed Htpim and 5-nitroisophthalic acid ($H_2\mathbf{L}$) by a solvothermal technique based on the following considerations: (1) the $H_2\mathbf{L}$ ligand contains two carboxylate groups and

---

* Corresponding authors. Fax: +86 372 2900040.
E-mail addresses: jjwang@aynu.edu.cn (J.-J. Wang), shiyunfeng2009@gmail.com (Y.-F. Shi).

http://dx.doi.org/10.1016/j.poly.2016.07.006
0277-5387/

substituted group $-NO_2$, promising rich coordination modes and different geometric and electronic effects to achieve diverse structures with interesting topology and tune framework stability and adsorption properties; (2) Htpim based Ln MOFs remain largely unexplored, which offers us a good opportunity to exploit this domain with the aim of discovering novel Ln-based MOFs with N-donor ligand; (3) H_2**L** and Htpim ligands, possessing electron conjugate systems, may be good chromophores and act as magnetic mediators and/or luminescent sensitizers via the "antenna effect" in the Ln-based complexes.

Considering all the aspects stated above, two novel Ln-based extended MOFs with protonated Htpim (H_3tpim) as templates have been synthesized and characterized: $\{[H_3tpim][Ln_2(\mathbf{L})_4(H_2O)]\}_n$ [Ln = La (**I**), Nd (**II**)]. In addition, the luminescent properties of the complexes have also been investigated in the solid state.

2. Experimental

All reagents and solvents for synthesis were commercially available and used as received or purified by standard methods prior to use. Elemental analyses (C, H and N) were performed on a Perkin-Elemer 240C analyzer. The IR spectra were recorded in the range of 4000–400 cm^{-1} on a Tensor 27 OPUS (Bruker) FT-IR spectrometer with KBr pellets. Thermogravimetric analysis (TGA) experiments were carried out on a NETZSCH STA 449F3 thermal analyzer from 40 to 800 °C under N_2 at a heating rate of 10 °C/min. The solid UV–Vis spectra were measured on UV25500 UV–VIS-NIR Spectrophotometer (SHIMADZU Corp.). Emission spectra in solid state at room temperature were recorded on a Cary Eclips fluorescence spectrophotometer.

2.1. $\{[H_3tpim][La_2(\mathbf{L})_4(H_2O)]\}_n$ (**I**)

A mixture of H_2**L** (106 mg, 0.50 mmol), Htpim (36 mg, 0.12 mmol) and $La(NO_3)_3 \cdot 6H_2O$ (95 mg, 0.25 mmol) was dissolved in 2 mL DMF and 4 mL aqueous solution. The resultant solution was sealed in a Teflon-lined stainless autoclave and heated to 160 °C. After keeping in these conditions for 3 days, light yellow single crystals suitable for X-ray analysis were obtained after cooling to room temperature. Yield: ~30% based on H_2**L** (54 mg). Elemental *Anal.* Calc. (%) for $C_{50}H_{29}N_9O_{25}La_2$: C, 41.87; H, 2.04; N, 8.80; found: C, 41.99; H, 2.21; N, 8.47%. IR (KBr pellet, cm^{-1}): 3365*s*(*br*), 2364*s*, 1868*w*, 1774*w*, 1732*w*, 1676*m*, 1615*s*, 1603*s*, 1560*s*, 1449*s*, 1382*s*, 1346*s*, 1205*w*, 1141*w*, 1107*w*, 1089*w*, 1003*w*, 966*w*, 931*w*, 887*w*, 838*w*, 795*m*, 734*m*, 714*s*, 666*w*, 604*w*, 532*w*, 447*w*, 426*w*.

2.2. $\{[H_3tpim][Nd_2(\mathbf{L})_4(H_2O)]\}_n$ (**II**)

The same procedure as that for **I** was used for this complex except that $La(NO_3)_3 \cdot 6H_2O$ was replaced by $Nd(NO_3)_3 \cdot 6H_2O$. Yellow single crystals suitable for X-ray analysis were obtained. Yield: ~20% based on H_2**L** (36 mg). Elemental *Anal.* Calc. (%) for $C_{50}H_{29}N_9O_{25}Nd_2$: C, 41.70, H, 2.03, N, 8.76; found: C, 41.93, H, 2.20, N, 8.60%. IR (KBr pellet, cm^{-1}): 3293*s*(*br*), 2365*s*, 1866*w*, 1779*w*, 1726*w*, 1683*m*, 1618*s*, 1602*s*, 1563*s*, 1455*s*, 1378*s*, 1346*s*, 1205*w*, 1139*w*, 1107*w*, 1085*w*, 1009*w*, 966*w*, 933*w*, 879*w*, 835*w*, 792*m*, 737*m*, 716*s*, 661*w*, 607*w*, 531*w*, 444*w*, 422*w*.

2.3. X-ray powder diffraction

The X-ray powder diffraction patterns (XRPD) of complexes **I** and **II** were recorded on a Rigaku D/Max-2500 diffractometer, operated at 40 kV and 100 mA, using a Cu-target tube and a graphite monochromator. The intensity data were recorded by continuous scan in a $2\theta/\theta$ mode from 5° to 40° with a step size of 0.02° and a scan speed of 8° min^{-1}.

2.4. X-ray crystallographic data

Single-crystal X-ray studies for complexes **I** and **II** were performed on a Bruker APEX II CCD diffractometer at 293(2) K. The determinations of unit cell parameters and data collections were performed with Mo Kα radiation with radiation wavelength of 0.71073 Å by using the ω-scan technique. The program SAINT [24] was used for the integration of the diffraction profiles. Semi-empirical absorption corrections were applied using the SADABS program [25]. All the structures were solved by direct methods using the SHELXS program of the SHELXTL package and refined with SHELXL [26]. Metal atoms in each complex were located from the E-maps, and other non-hydrogen atoms were located in successive difference Fourier syntheses and refined with anisotropic thermal parameters on F^2. The hydrogen atoms were added theoretically, riding on the concerned atoms and refined with fixed thermal factors. Crystallographic information for complexes **I** and **II** is summarized in Table 1. Selected bond distances are listed in Table 2.

3. Results

3.1. Synthesis

Solvothermal synthesis has recently been proven to be a useful technique in the preparation of MOF materials, though its mechanism is not yet completely clear. Up to now, some Ln(III) complexes with different organic templates have been synthesized and structurally characterized. Most of these complexes were synthesized under solvothermal conditions [27]. In a specific solvothermal process, many factors can affect the formation and crystal growth of products, such as counteranions [28], the pH value of the reaction solution [29], temperature [30] and solvent system [31]. Complexes **I** and **II** were obtained by solvothermal reactions of the corresponding $Ln(NO_3)_3$ with Htpim and H_2**L** ligands. In our case, the addition of Htpim is the key to the

Table 1
Crystal data and structure refinement summary for complexes **I** and **II**.

	I	**II**
Formula	$C_{50}H_{29}N_9O_{25}La_2$	$C_{50}H_{29}N_9O_{25}Nd_2$
Formula weight	1433.64	1444.30
Crystal system	triclinic	triclinic
Space group	$P\bar{1}$	$P\bar{1}$
Unit cell dimensions		
a (Å)	10.714(2)	10.637(2)
b (Å)	15.599(3)	15.543(3)
c (Å)	17.739(4)	17.656(4)
α (°)	71.82(3)	72.04(3)
β (°)	75.14(3)	75.44(3)
γ (°)	76.64(3)	77.33(3)
V (Å^3)	2685.6(9)	2655.6(9)
Z	2	2
ρ_{calcd} (g cm^{-3})	1.773	1.806
$F(000)$	1412	1424
μ (mm^{-1})	1.667	2.032
Collected reflections	24417	26166
Unique reflections	13293	12999
R_{int}	0.0258	0.0451
Goodness-of-fit (GOF)	0.928	0.927
R_1 ($I > 2\sigma(I)$)[a]	0.0305	0.0407
wR_2 (all data)[b]	0.0779	0.0910
$\rho_{maximum}/\rho_{minimum}$ (e Å^{-3})	0.762/−0.555	1.009/−0.967

[a] $R = \Sigma(||F_o| - |F_c||)/\Sigma|F_o|$.

[b] $wR = [\Sigma w(|F_o|^2 - |F_c|^2)^2/\Sigma w(F_o^2)^2]^{1/2}$, where F_o = observed and F_c = calculated structure factors, respectively.